

# Plasma-Degradation of Dinitrophenols and Interpretation by the Molecular Orbital Theory<sup>\*)</sup>

Hiroshi OKAWA, Hiroki KURODA, Keiko HIRAYAMA-KATAYAMA<sup>1)</sup>, Shin-Ichiro KOJIMA<sup>2)</sup> and Tetsuya AKITSU<sup>1)</sup>

*Happy Science University, 4427-1 Hitotsumatsu-Hei, Chosei, Chiba 299-4325, Japan*

<sup>1)</sup>*University of Yamanashi, 4-3-11 Takeda, Kofu, Yamanashi 400-8511, Japan*

<sup>2)</sup>*Kyushu University, Fukuoka 812-8581, Japan*

(Received 8 January 2019 / Accepted 9 March 2019)

The advanced oxidation of 2, 4 - dinitrophenol (DNP), 2, 5 - DNP, and 3, 4 - DNP in aqueous solution has been investigated using a multi-gas, dielectric barrier discharge, and the degradation was measured by high performance liquid chromatography (HPLC). The acceleration of the advanced-oxidation has been investigated by the combination of the anion exchange polymer. The degradation pathway was suggested involving a rapid detachment of the nitro group followed by a slow opening of the aromatic-ring. The hydroxyl radical and the excited hydroxyl anion are responsible for the primary attack of the DNP with the production of dihydroxy-nitrobenzenes. The attack of hydroxyl radical occurs at the benzene ring carbon activated by the presence of a phenolic OH group and a nitro group. The reaction is dominated by a pseudo-first order kinetic reaction. The degradation process is interpreted using Molecular Orbital Theory.

© 2019 The Japan Society of Plasma Science and Nuclear Fusion Research

Keywords: dielectric barrier discharge, aromatic compound, dinitrophenol, advanced oxidation, molecular orbital theory, advanced oxidation

DOI: 10.1585/pfr.14.3406071

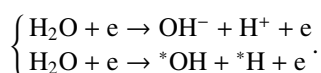
## 1. Introduction

The advanced oxidation is attracting attentions as the technology for pollution of drinking-water reservoirs by aromatic compounds. In recent work, we reported the decomposition of the aromatic compound in comparison using working gases: argon, nitrogen, oxygen, and air (20% oxygen and 80% nitrogen mixture) [1]. In this work, we describe the degradation in dielectric barrier discharge plasma in air. The degradation of three types of dinitrophenols (DNP): 2, 4 - DNP; 2, 5 - DNP; and 3, 4 - DNP will be compared. Chemical reaction between the organic compound and the active component is discussed with Molecular Orbital Theory. In this proceedings, we present the summary of the experimental part of this work.

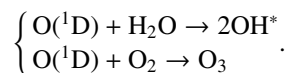
## 2. Materials and Methods

Lukes *et al.* [2] reported the enhancement of <sup>\*</sup>OH radical production and O<sub>3</sub> decomposition in the presence of N<sub>2</sub> molecules in humid air, through the following reactions.

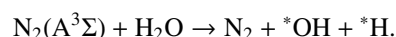
*Dissociation and ionization generating OH anion and radicals*



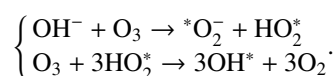
*Reactions including excited oxygens*



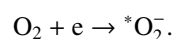
*Reactions including metastable state of nitrogen molecules*



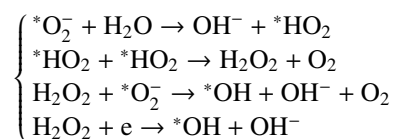
*Inhibition of O<sub>3</sub> production and enhancement of OH\* formation:*



*Production of superoxide: Oxygen molecule is the primary acceptor of electrons and forms <sup>\*</sup>O<sub>2</sub><sup>-</sup>*



*Production of hydroxyl radicals:*



DNP + {<sup>\*</sup>OH + OH<sup>-</sup>} → Produced system.

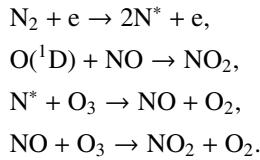
Super oxide is highly reactive anions and form hydrogen-peroxide in the chain reaction. Hydroxyl radical and hydroxyl anion are produced in the dissociation of hydrogen peroxide by the electron collision in the discharge area as

author's e-mail: hiroshi-okawa@happy-science.university

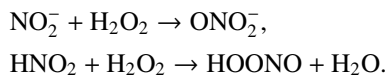
<sup>\*)</sup> This article is based on the presentation at the 27th International Toki Conference (ITC27) & the 13th Asia Pacific Plasma Theory Conference (APPTC2018).

well as by the decomposition of ozone in water reactions. Reactions in air with humidity, one of the merits is the suppression of ozone generation.

*Nitrogen reactions including the ozone quench generating the excited state of nitrogen and NO<sub>x</sub>*



*Reactions related to NO<sub>2</sub><sup>-</sup> and nitrous acid, related to the production of nitrite ions and ONOO, peroxonitrite:*



Peroxonitrite ONO<sub>2</sub><sup>-</sup> is attracting attentions in the advanced oxidation, but the effect is not fully-understood. NO and NO<sub>2</sub> cause the electrophilic replacement reaction with hydrogen atoms in the benzene ring. In this experiment, the reverse reaction was reduced by controlling the temperature of the solution and the anion-exchange using gel-type poly-styrene-base alkalized trimethyl-ammonium polymer. (Sanei Chemical, Kumamoto, Japan)

Figure 1 shows the dielectric barrier discharge plasma source. This plasma source consists of a quartz tube,

3.0 mm outer diameter and 1.4 mm inner diameter and W/Re (6%) wire, 0.6 mm in diameter coaxially located. These components are assembled with a Teflon Cajon-type elbow coupler. The quartz tube of the plasma source is immersed in the water-solution, which is connected to the ground electrode through the capacitive coupling. Figure 2 shows the estimation of the discharge power on the basis of the Q versus V Lissajous curve. The total capacitance C<sub>PR</sub> includes the dielectric barrier discharge in the gas-region and the capacitance across the water region.

When monitoring capacitor is 4200 pF, for example, the one cycle along the contour, 10<sup>-7</sup> C along the vertical axis multiplied by 5 × 10<sup>3</sup> V along the horizontal axis is equivalent to 5 × 10<sup>-4</sup> J/cycle.

The electrical power input at 16.5 kHz is 8.25 W. The power source is a quasi-sinusoidal wave inverter, 16.69 - 16.94 kHz, 8.48 - 7.84 kV, peak to peak, (Type 10AC-24, Logy Electronics, Tokyo, Japan). Table 1 shows the dependence of the output voltage on the control voltage (DC input) and the discharge power. When the plasma source was operated at the control voltage of 13 volts and higher, the discharge formed transfer mode glow discharge.

The discharge voltage was measured with P-3000 high voltage probe and the discharge current was measured with TCP312 current probe clamped to the ground side wire with preamplifier TCPA300 (Tektronix, Beaverton, USA)

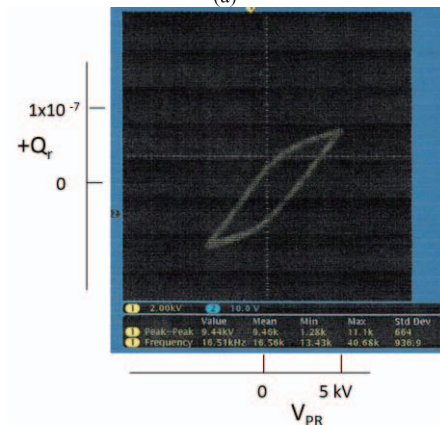
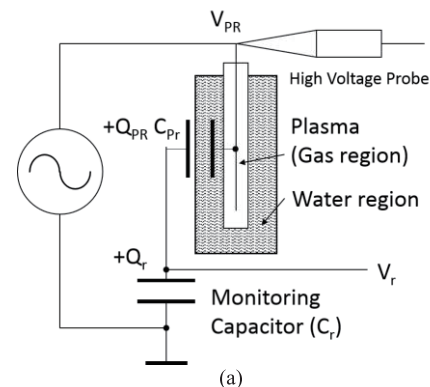
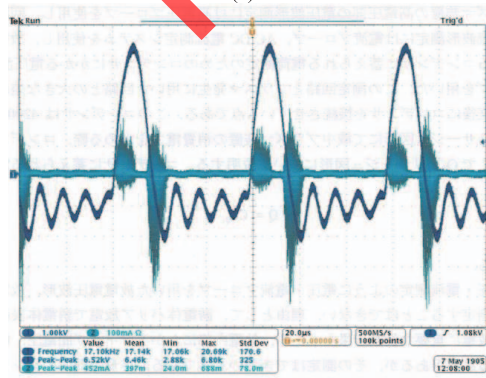
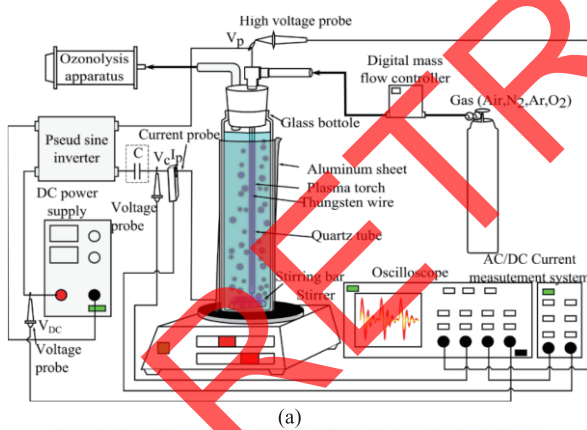


Fig. 1 Experimental setup; (a) Layout; (b) Waveforms, voltage: 1 kV/div, current: 100 mA/div. 6.5 kV and 452 mA peak-to-peak.

Fig. 2 Typical waveforms and the Q versus V Lissajous curve. (a) Measurement circuit; (b) Lissajous curve.

Table 1 Estimation of the discharge power.

Discharge mode	Parameters	
	Control voltage (V)	Power (W)
Dielectric Barrier Discharge	6.45	3.69
	8.66	6.96
	9.46	9.48
	11.0 a	12.36
Glow discharge	>13	

Frequency: 16.34 – 16.94 kHz.

The concentration of the remaining DNP was measured with liquid chromatograph, L-6000 (Hitachi Co., Japan) equipped with UV-detector, L-4200, (Hitachi Co., Japan) with column Waters X-bridge 4.6, 250 mm. TOC measurement was carried out by TOC-LCSH/CSN and auto sampler, ASI-L, (Shimadzu Co., Japan) Ion chromatography for anion detection, ICS-1100 (Dionex), with column IonPac AS22 (Dionex,) and guard column, IonPac, AG22 (Dionex). In the ion chromatography, the detector was replaced to the electro-conductive detector. The reproducibility and the anion exchange was examined using liquid chromatograph, HPLC Prominence-I LC-2030Plus, (Shimadzu Co., Japan) installed with UV - detector and a reverse mode column: Xbridge C-18, 5 μm.

### 3. Experimental Result

Figure 3 shows the concentration of DNP and TOC (Total Organic Carbon). TOC is detected as CO<sub>2</sub> from the solid body of the incinerated dried solution. The detachment of NO<sub>2</sub> is completed in 10 minutes. However, longer process is needed for the reduction of TOC, which remains almost 70 percent of the initial concentration. This result indicates the production of the intermediate product, such as hydroquinone. Figure 4 shows the evolution of the concentration of NO<sub>3</sub><sup>-</sup> and pH. The efficiency of the plasma degradation is compared for dinitrophenols: 2, 4 - DNP, 2, 5 - DNP, and 3, 4 - DNP. Table 2 is the TOC, pH, the concentration of DNP and NO<sub>3</sub><sup>-</sup> after 60 minutes.

After 20 minutes of the plasma injection, the pH value becomes lower than 4, due to the accumulation of nitric acid. Comparing with the initial phase, the concentration of hydroxyl anion may show proportional reduction in the ionization equilibrium. The decomposition reaction is supply dominated by excited OH anions and OH\* which are supplied from the plasma region. The influence of the change in the ionization balance may be negligible. On the other hand, the accumulation of nitric acid may cause the reverse exchange reaction. Nitric anion was reduced by the anion exchange by gel type poly-styrene base alkaliized trimethyl-ammonium polymer. Apparently, the final concentration of NO<sub>3</sub><sup>-</sup> exceeds the original concentration of the nitro-group, and the solution shows acidity. The weight of nitric anion is calculated. If two nitrogen atoms are converted to NO<sub>3</sub><sup>-</sup>, one oxygen comes from the working gas. From the molar ratio;

$$98/184.106 \times [20 \text{ mg/L}] = 10.646 \text{ mg/L.}$$

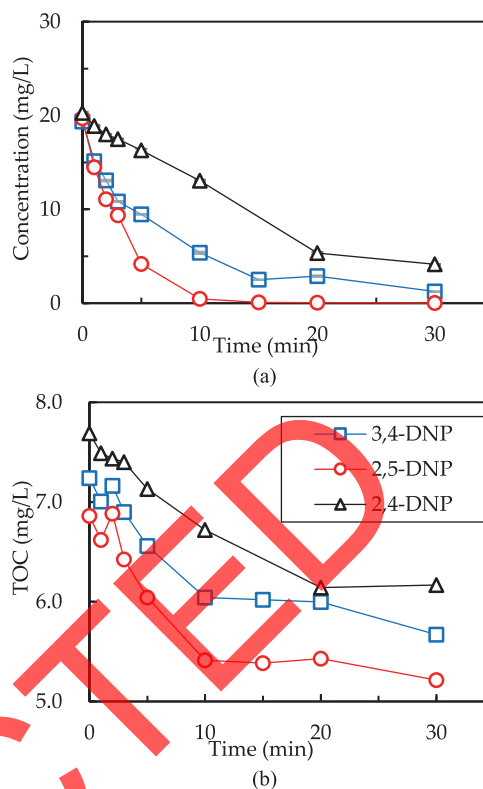


Fig. 3 Experimental results; (a) HPLC; (b) TOC.

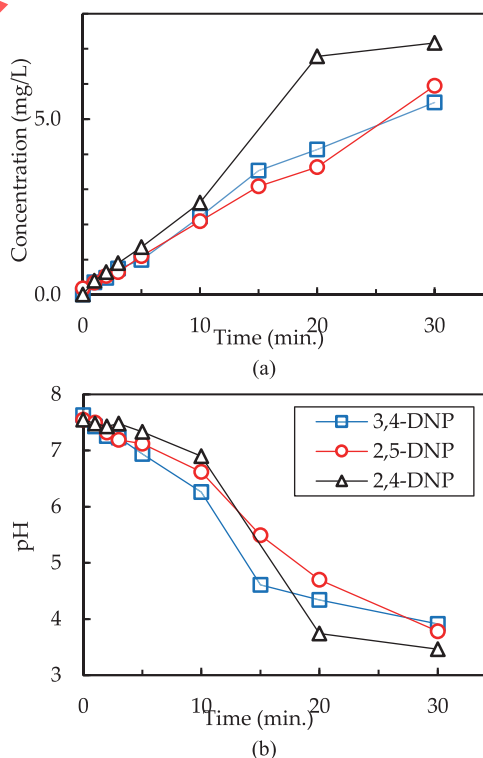


Fig. 4 Ion chromatography and pH measurement; (a) Concentration of NO<sub>3</sub><sup>-</sup> anion; (b) pH.

The increase in NO<sub>3</sub><sup>-</sup> anion is attributed to the oxidation in the working gas. This acid solution is not suitable for the release. Figure 5 shows the evolution of the concentration.

Table 2 Concentration, TOC and pH\*.

DNP specie	Concentration (mg/L)			pH
	TOC	DNP	NO <sub>3</sub> <sup>-</sup>	
2, 5 DNP	4.310*	0	20.6	3.5
3, 4 DNP	5.139	0	19.0	3
2, 4 DNP	5.117	0.002	19.6	2.99

\*pH meter: HM-25R (DKK - TOA Corporation, Japan).

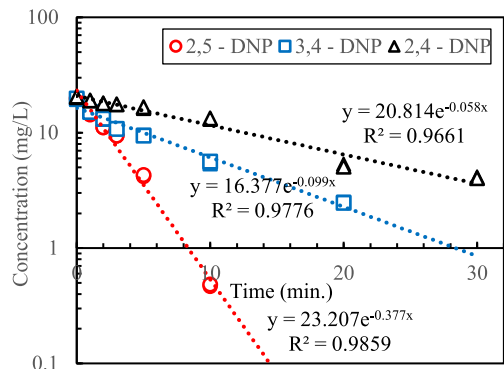


Fig. 5 Exponential recurrence function.

Table 3 Coefficients.

DNP specie	Recurrent function		
	a	b	R-squared
2, 4 - DNP	0.058	0.04	0.9661
3, 4 - DNP	0.099	-0.200	0.9776
2, 5 - DNP	0.377	0.148	0.9859

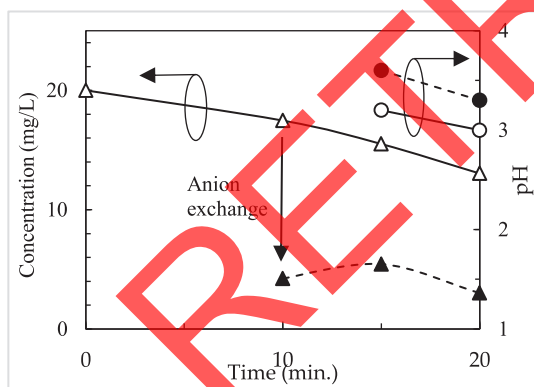


Fig. 6 Shortcut of degradation by gel type poly-styrene base alkalized trimethyl-ammonium polymer.

The recurrence function can be expressed with following form (Table 3):

$$\ln\left(\frac{C_t}{C_0}\right) = -at - b, C_0 = 20 \text{ [mg/L]}.$$

The plasma process increases neutral materials in the object, even if our aim is the ionized or excited radicals. The anion exchange polymer captured the excessive material, NO<sub>3</sub><sup>-</sup> and exchanged with hydroxyl anion OH<sup>-</sup>. Figure 6 shows the shortcut of the degradation using anion exchange for 2, 4 - DNP.

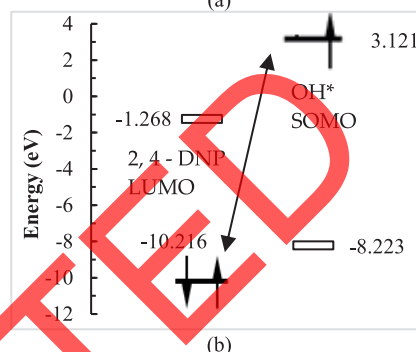
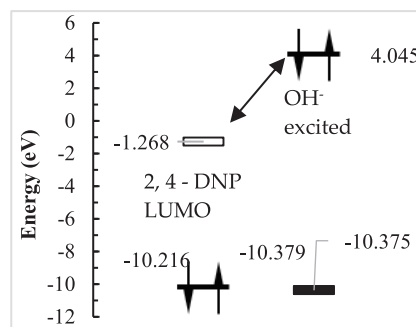


Fig. 7 Energy diagram of LUMO and HOMO state of the starting system (a) excited hydroxyl anion; (b) hydroxyl radical.

### 4. Discussions

The effects of the frontier electrons in the Highest Occupied Molecular Orbital (HOMO) of the active component, OH anion and OH\* radical and the Lowest Unoccupied Molecular Orbital (LUMO) of the target compound determines the reaction mechanisms, using Biomedical CACHE [3, 4]. The starting system of 2, 4 - DNP shows LUMO energy of -1.268 eV, and HOMO energy -10.210 eV. The excited OH<sup>-</sup> anion shows LUMO energy 4.045 eV and HOMO energy -10.375 eV. This reaction is directed to the nucleophilic reaction. OH\* radical shows singly occupied molecular orbit (SOMO) energy of 3.121 eV, and this reaction is directed to electrophilic reaction directed to the HOMO level, -10.210 eV. Figure 7 shows the energy diagram of 2, 4 DNP with excited hydroxyl anion and hydroxyl radical. Comparing the energy state of OH anion (in NaOH) with 2, 4 - DNP. This OH<sup>-</sup> anion shows HOMO level (-2.61 eV) lower than the LUMO level (-1.268 eV) of 2, 4 - DNP. The difference is necessary for the excitation, 1.342 eV. The produced system consists of 1, 2 - OH 4 - nitrobenzene and NO<sub>3</sub> anion of HNO<sub>3</sub>. Figure 8 shows the energy diagram of the produced system. Although the quantum-chemical calculation indicates that the exchange reaction is exothermic reaction including the production system, this reaction was not observed.

This reaction is supply-dominated by OH radicals and anions excited in the plasma region. Figure 9 shows the 3D model of the frontier electron density distribution. The nucleophilic reaction by OH anion targets the negative

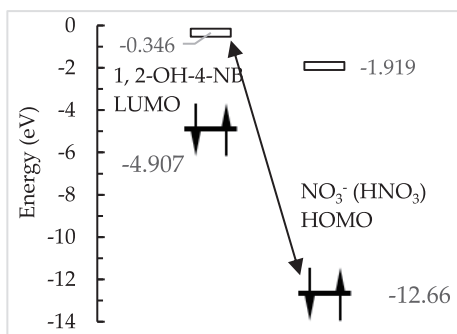


Fig. 8 Energy diagram of the produced system.

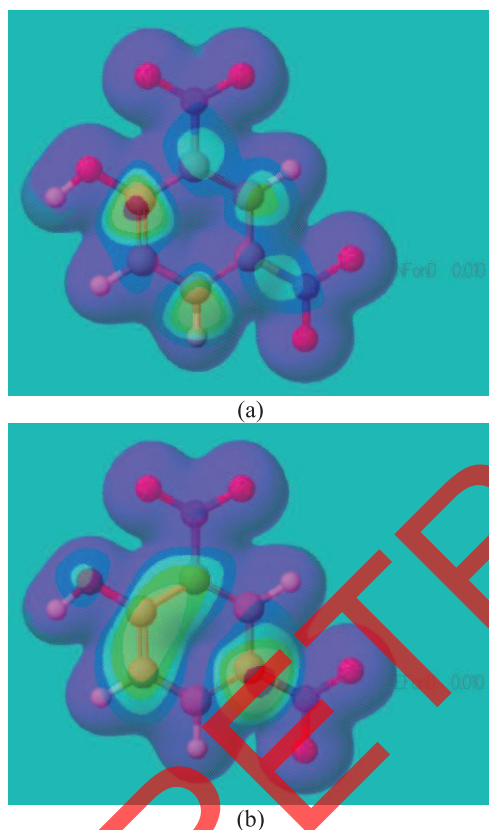


Fig. 9 Frontier electron density of 2, 4 - DNP; (a) Nucleophilic reaction; (b) Electrophilic reaction.

space charge of electron injected by OH system. Similarly, the electrophilic reaction by OH radical targets the positive space charge of electron depletion around NO<sub>2</sub> system. Appendix shows the 3D model of iso-surface of the frontier electron density of the LUMO state and the HOMO state, the energy is -1.268 eV and -10.210 eV, respectively.

### 5. Conclusion

Plasma-degradation of the dinitrophenyl was studied using a compact dielectric barrier discharge in a quartz tube, immersed into the liquid surface. As the dielectric barrier discharge can be operated at low electric power, this

method is a feasible solution for the water remediation. In the air-plasma treatment, the accumulation of nitric anion was, solved and realized by shorter solution using the anion exchange. The degradation of the nitro system was interpreted by the Molecular Orbital Theory. The LUMO energy level of the organic compound is lower than the HOMO energy level of the active component, OH<sup>-</sup>. The reaction proceeds to the detachment of nitric anion, and the reverse reaction shows higher activation energy.

### Acknowledgement

This research received a fund from Future Science Institute, Tokyo, Japan. The authors express their gratitude to Mr. Kento Nakai and Mr. Kenya Yabu.

### Appendix A

2-D and frontier electron density model of 2, 4 - DNP [5].

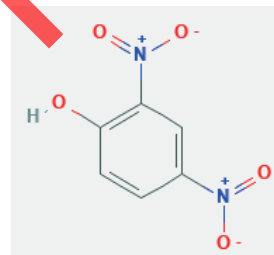


Fig A. 1 2-D structures of 2, 4 - DNP.

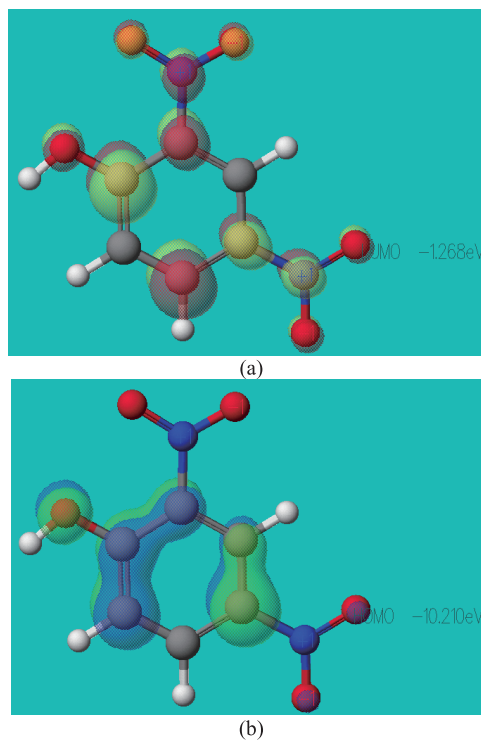


Fig A. 2 LUMO and HOMO energy state of 2, 4 - DNP.

- [1] S. Kojima, K. Katayama-Hirayama and T. Akitsu, *World Journal of Engineering and Technology* **4**, 423 (2016). <http://DOI.ORG/10.4236/wjet.2016.43042/>
- [2] P. Lukes and B.R. Locke, *Industrial and Engineering Chemistry Research*, **44**(9), 2921 (2005). <https://DOI.ORG/10.1021/ie0491342>
- [3] *Biomedical CAChe 6.0 Users Guide*, 2003, Fujitsu.
- [4] K. Somekawa, *Molecular Orbital Calculation of Organic Molecules and the Application*, (Kyushu University Press, Fukuoka, Japan, 2013) ISBN 978-4-7985-0089-8.
- [5] PUBCHEM [https://pubchem.ncbi.nlm.nih.gov/compound/3\\_4-dinitrophenol#section=2D-Structu](https://pubchem.ncbi.nlm.nih.gov/compound/3_4-dinitrophenol#section=2D-Structu)

RETRACTED